Fractal Dimensional Analysis of Optical Coherence Tomography Angiography in Eyes With Diabetic Retinopathy

Sarwar Zahid,[1] Rosa Dolz-Marco,[2,3] K. Bailey Freund,[1–4] Chandrakumar Balaratnasingam,[1–3,5] Kunal Dansingani,[2,3,6] Fatimah Gilani,[2,3] Nitish Mehta,[1] Emma Young,[1] Meredith R. Klifto,[1] Bora Chae,[1] Lawrence A. Yannuzzi,[1–4] and Joshua A. Young[1]

[1]Department of Ophthalmology, New York University Langone Medical Center, New York, New York, United States
[2]Vitreous Retina Macula Consultants of New York, New York, New York, United States
[3]LuEsther T. Mertz Retinal Research Center, Manhattan Eye, Ear, and Throat Hospital, New York, New York, United States
[4]Department of Ophthalmology, Edward S. Harkness Eye Institute, Columbia University College of Physicians and Surgeons, New York, New York, United States
[5]Department of Physiology and Pharmacology, Lions Eye Institute, University of Western Australia, Perth, Australia
[6]Truhlsen Eye Institute, University of Nebraska Medical Center, Omaha, Nebraska, United States

Correspondence: Joshua A. Young, New York University Langone Medical Center, Department of Ophthalmology, 462 First Avenue, NBV 5N18, New York, NY 10016, USA;
jyoungmd@gmail.com.

Submitted: March 29, 2016
Accepted: August 4, 2016

Citation: Zahid S, Dolz-Marco R, Freund KB, et al. Fractal dimensional analysis of optical coherence tomography angiography in eyes with diabetic retinopathy. *Invest Ophthalmol Vis Sci*. 2016;57:4940–4947. DOI:10.1167/iovs.16-19656

Purpose. We used fractal dimensional analysis to analyze retinal vascular disease burden in eyes with diabetic retinopathy using spectral-domain optical coherence tomography angiography (OCTA).

Methods. A retrospective study was performed of 13 eyes with diabetic retinopathy without diabetic macular edema and 56 control eyes. Optical coherence tomography angiography images were acquired using the RTVue XR Avanti. Automated segmentation was obtained through the superficial and deep capillary plexuses for each eye. Grayscale OCTA images were standardized and binarized using ImageJ. Fractal box-counting analyses were performed using Fractalyse. Fractal dimensions (FD) as well as software-generated vascular density analyses of the superficial and deep capillary plexuses were compared between diabetic and control eyes using 2-tailed *t*-tests and 1-way multivariate ANOVA (MANOVA) analyses.

Results. The superficial and deep plexuses from diabetic and control eyes were analyzed. The average FD for diabetic eyes was significantly lower than control eyes for the superficial ($P = 4.513 \times 10^{-3}$) and deep ($P = 2.653 \times 10^{-3}$) capillary plexuses. In diabetic eyes, the vascular density also was significantly reduced in the superficial ($P = 8.068 \times 10^{-5}$) and deep ($P = 3.120 \times 10^{-6}$) capillary plexuses. One-way MANOVA showed a significant difference between diabetic and control eyes.

Conclusions. The OCTA FD is significantly reduced in the superficial and deep capillary plexuses in eyes with diabetic retinopathy. Applying fractal analysis to OCTA imaging holds the potential to establish quantitative parameters for microvascular pathology.

Keywords: optical coherence tomography angiography, diabetic retinopathy, angiography, optical coherence tomography, image analysis

Sensitive and objective parameters to monitor disease severity have immediate clinical value in helping guide therapy to patients who will benefit most. Specifically, for microvascular diseases, such as diabetes, prior work on automated grading of disease severity have used fundus photography and spectral-domain optical coherence tomography (SD-OCT), which provides helpful qualitative information about retinal pathology.[1–5] However, quantitative representations of microvascular disease, aside from quantification of diabetic macular edema (DME) using SD-OCT, have been more challenging.

Fractals are patterns found in nature and biological systems that demonstrate the same level of complexity and general pattern regardless of the scale on which they are measured.[6] Fractal geometric analysis is a non-Euclidian mathematical framework used to assess the fractal nature of biological structures. The degree of complexity of such a shape is described by the parameter "fractal dimension" (FD) whose value is less than the spatial dimension subtended by the pattern. Thus, a fractal pattern in two-dimensional space will have a FD between 1 and 2 and a fractal pattern in three-dimensional space will have a FD between 2 and 3. A simple method to measure the FD of a two-dimensional shape, and the method used in this study, is to divide the two-dimensional pattern into a grid of squares (box-counting). A count is made of the number of squares subtended by the pattern; this count is repeated and the size of the squares of the grid is reduced. This method allows for a calculation of a FD, which is a mathematical parameter that describes the complexity of a biological structure.

Fractal analysis of the retinal vasculature in color fundus photographs and fluorescein angiographic images has been

Investigative Ophthalmology & Visual Science

attempted with limited success by researchers as early as 1990.[7–10] Many of these studies have shown that the normal retinal vasculature also exhibits fractal geometry and demonstrates a FD of approximately 1.7.[11,12] Given that microvascular diseases, such as diabetes and hypertension, result in changes to the microvascular architecture,[13] it may be hypothesized that the loss of smaller vessel branches would reduce the FD. Indeed, several studies of color photographs and fluorescein angiography (FA) have shown that diabetic eyes demonstrate a reduced FD.[14–16] While FA allows anatomic differentiation and visualization of abnormalities based on timing, there is limited evaluation of the peripapillary or deeper retinal capillary networks; staining and vascular leakage also further undermine resolution. In contrast, SD-OCT angiography (OCTA) has the potential to image different layers of the retinal vasculature based on the presence or absence of flow.[17,18] Although OCTA remains a promising new modality, OCTA images have thus far been interpreted largely qualitatively.[19,20] Given the more detailed imaging of each retinal vascular layer possible with OCTA compared to fundus photographs and FA, these images are well-suited for fractal analysis and may shed new insights and quantifiable parameters for microvascular diseases.

We report the application of fractal geometric analysis to OCTA imaging in controls compared to patients with any degree of diabetic retinopathy without DME. Given the predilection of diabetic retinopathy to preferentially affect smaller vessel branches, we hypothesized that the FD would be reduced in the superficial and deep capillary networks. The combination of anatomically representative OCTA data and fractal analysis holds the potential to establish quantitative disease parameters for microvascular pathology.

Methods

Patient Population

This retrospective observational case series was approved by the Institutional Review Board of the Manhattan Eye, Ear and Throat Hospital/North Shore Long Island Jewish Hospital, New York, NY, USA. It complied with the Health Insurance Portability and Accountability Act of 1996 and followed the tenets of the Declaration of Helsinki. Patients were recruited from the private practices of the Vitreous, Retina, Macula Consultants of New York (Manhattan and Brooklyn offices) between September 2014 and June 2015. Inclusion criteria were age greater than 18 years, history of diabetes mellitus (type 1 or 2), presence of mild nonproliferative diabetic retinopathy to proliferative diabetic retinopathy without evidence of DME on structural SD-OCT, and good quality OCTA images (signal strength score greater than 53) and no motion artifacts to degrade the interpretability of the image. Patients with a history of posterior uveitis, retinal artery occlusion or retinal vein occlusion were excluded from this study; those with a history of prior focal or grid laser treatment were excluded only if there was associated macular atrophy on SD-OCT. Patients with DME or atrophy shown on structural SD-OCT were excluded given the potential for OCTA imaging artifacts.

Clinical data collected included basic patient demographic information, Snellen best-corrected visual acuity (BCVA), degree of diabetic retinopathy, and past ocular treatment. Conventional fundus photography (Topcon America, Paramus, NJ, USA), ultrawide-field photography (Optos, Marlborough, MA, USA), and high-resolution SD-OCT (Heidelberg Spectralis, Heidelberg Engineering, Heidelberg, Germany) images were reviewed for each patient. Optical coherence tomography angiography imaging was performed using the RTVue XR Avanti (Optovue, Inc., Fremont, CA, USA); the 3×3 mm image acquisition area centered on the fovea was selected for all patients. The Optovue takes 304×304 volumetric A-scans at 70,000 A-scans per second, with flow being detected using the split-spectrum amplitude-decorrelation angiography (SSADA) algorithm. The two-dimensional flow maps are rendered as 304×304 pixels in 8-bit grayscale. Dense horizontal and vertical raster cubes are acquired and combined by a proprietary algorithm to reduce motion artifacts. A total of 29 volunteer subjects without a history of diabetes or any ocular diseases, who had unremarkable clinical examinations, also underwent OCTA imaging as described above.

OCTA Image Processing

Using the default automated segmentation boundaries, separate flow maps were obtained of the superficial and deep capillary plexuses for each eye, resulting in two images per eye (Figs. 1A, 1D). The grayscale OCTA images were standardized, cropped, and binarized using ImageJ (National Institutes of Health [NIH], Bethesda, Maryland, USA; Figs. 1B, 1E).[21]

The following macro was constructed and applied within ImageJ to all OCTA images:

```
setAutoThreshold("Default dark");
setThreshold(0.0504, 0.1395);
setOption("BlackBackground", false);
run("Convert to Mask").
```

Fractal Analysis

The box-counting method was used to calculate an FD for each image. In this method, a count is made of the number of squares subtended by pattern in an image; this count is repeated as the size of the squares of the grid is reduced. The box-counting FD calculated by this method may be used to compare the degrees of complexity among different vascular patterns, in our case between normal and diabetic OCTA images.

The box-counting FD is given by the relationship

$$D_S = \frac{\log N_r}{\log r^{-1}}$$

in which D_S is the fractal dimension as measured by box counting and N_r is the number of boxes subtended by boxes of ratio r.[22]

Fractal dimensional box-counting analyses were performed using Fractalyse (ThéMA, Besançon Cedex, France) resulting in an FD value for each image (Figs. 1C, 1F).[23]

The average of FD values of the superficial and deep capillary plexuses were compared between diabetic and control eyes using 2-tailed heteroscedastic *t*-tests. The Avanti software-generated automated vascular density analysis (which assesses the proportion of pixels subtended by vessels from the total number of pixels in a binary image obtained from the en face OCTA grayscale image) also was obtained for the superficial and deep plexuses of each eye and compared between diabetic and control eyes. One-way multivariate ANOVA (MANOVA) was used to determine if there was a global difference between diabetic and control eyes based on OCTA quantitative parameters (superficial FD, deep FD, superficial vessel density, and deep vessel density). Statistical analyses were performed using SPSS v.22.0 (IBM Corp., Armonk, NY, USA). A P value less than 0.05 was considered statistically significant.

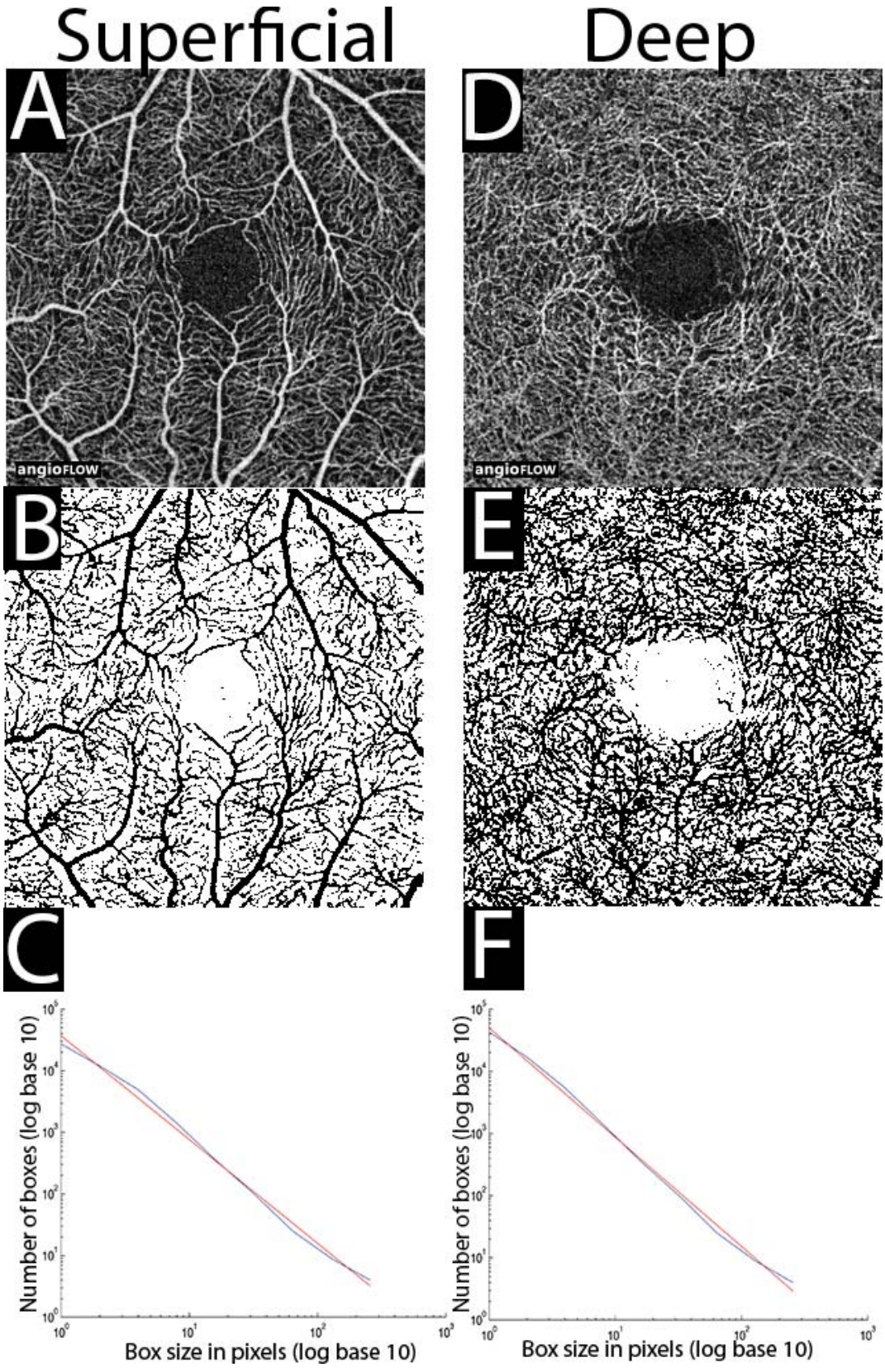

FIGURE 1. Left eye from a 30-year-old male in the control group. Superficial capillary plexus (*left column* from *top* to *bottom*): (**A**) Spectral-domain optical coherence tomography angiography image of the segmented through the superficial capillary plexus. (**B**) Spectral-domain optical coherence tomography angiography image after standardization, cropping, and binarization. (**C**) Output of fractal analysis of the image in (**B**); the *blue curve* represents actual OCTA data for this image, while the *red line* displays the closest fitting fractal log-log line. The *x*-axis indicates the log base 10 of the size of the boxes in pixels, while the *y*-axis indicates the log base 10 of the number boxes subtending the OCTA pattern. Since a linear

relationship in the log-log plot is an indication of perfect self-similarity, high correlation demonstrates a high degree of self-similarity in OCTA pattern. The FD for this image was determined to be 1.685. Deep capillary plexus (*right column* from *top to bottom*): (**D**) Spectral-domain optical coherence tomography angiography image segmented through the deep capillary plexus. (**E**) Spectral-domain optical coherence tomography angiography image after processing. (**F**) output of fractal analysis of the image in (**E**); the *blue curve* represents actual OCTA data for this image, while the *red line* displays the closest fitting fractal log-log line. The *x*-axis indicates the log base 10 of the size of the boxes in pixels, while the *y*-axis indicates the log base 10 of the number boxes subtending the OCTA pattern. Since a linear relationship in the log-log plot is an indication of perfect self-similarity, high correlation demonstrates a high degree of self-similarity in OCTA pattern. The FD for this image was determined to be 1.759.

Results

Fractal Dimension and Vascular Density in Control Eyes

We evaluated 56 eyes from 29 subjects, ranging in age from 25 to 60 years (mean, 32.27 years; SD, 6.71 years); all cases had a BCVA of 20/20. Optical coherence tomography angiography signal strength averaged 78.16. The average FD for the superficial capillary plexus was 1.638 (SD = 0.0452, range = 1.568–1.77). The average FD for the deep capillary plexus was 1.719 (SD = 0.0399, range = 1.624–1.794). Figure 2 demonstrates one example of the superficial (Figs. 2A, 2B) and deep (Figs. 2E, 2F) capillary plexus before (Figs. 2A, 2E) and after (Figs. 2B, 2F) processing. The average vascular densities in the superficial (Fig. 2C) and deep (Fig. 2G) capillary plexuses were 55.56% (SD = 1.69) and 60.58% (SD = 1.50), respectively.

Fractal Dimension and Vascular Density in Diabetic Eyes

We studied 13 diabetic eyes from 8 patients, ranging in age from 36 to 79 years (mean, 56.66 years; SD, 12.65 years) with a BCVA ranging from 20/20 to 20/60 (mean, 20/29). Of the 13 eyes, 5 eyes had mild nonproliferative diabetic retinopathy (NPDR), while the remaining 8 eyes had a quiescent proliferative diabetic retinopathy (PDR) with history of treatment with panretinal photocoagulation. Three of the eyes with quiescent PDR had a history of DME (now resolved) previously treated with intravitreal antivascular endothelial growth factor injections. None of the 13 eyes had active DME. The OCTA signal strength averaged 72.27. The superficial capillary plexus in diabetic eyes exhibited an average FD of 1.563 (SD = 0.0770, range = 1.434–1.698; Figs. 3A, 3B), while the deep capillary plexus showed an average FD of 1.5999 (SD = 0.113, range = 1.268–1.697; Figs. 3E–F). In diabetic eyes, the average vascular densities in the superficial and deep capillary plexuses were 48.22% (SD = 4.59; Fig. 3C) and 53.57% (SD = 3.21; Fig. 3G), respectively. There were no statistically significant differences between the 5 eyes with NPDR and 8 eyes with quiescent PDR ($P > 0.05$, 2-tailed heteroscedastic *t*-test).

Comparison of Fractal Dimensions and Vascular Density Between Diabetic and Control Eyes

The fractal dimension was significantly lower in diabetic eyes compared to control eyes for the superficial ($P = 4.513 \times 10^{-3}$) and deep ($P = 2.653 \times 10^{-3}$) capillary plexuses. The vascular density also was significantly reduced for the superficial ($P = 8.068 \times 10^{-5}$) and deep ($P = 3.120 \times 10^{-6}$) capillary plexuses. One-way MANOVA showed a significant difference between diabetic and control eyes when comparing all four parameters ($F_{[4,64]} = 36.1$, Wilk's $\lambda = 0.307$, partial $\eta^2 = 06.63$). Figure 4 demonstrates an example comparing a control and a diabetic eye.

Discussion

Our study takes advantage of the intrinsic fractal nature of retinal vascular branching. Given the predilection of diabetes to preferentially attenuate and affect smaller vessel branches, the fact that the FD is reduced in eyes with retinopathy is consistent with pathophysiology.[14,16] Evaluating OCTA imaging of the superficial and deep capillary plexuses, which is more representative of actual anatomy compared to previous fractal analyses of fundus photographs and fluorescein angiography, we showed significant reductions in the FD in diabetic eyes in the absence of DME.

Prior work on fractal analysis of the retinal vasculature has shown statistically significant reductions of the FD in patients with different stages of diabetic retinopathy using fundus photographs[14,16] and FA.[16] Other studies have reported the utility of fractal analysis to detect new vessels in proliferative diabetic disease, where the FD may increase.[24–26] However, given that these prior studies analyzed fundus photographs and FA images, the data analyzed were two-dimensional and vertically summated (with simultaneous visualization of multiple layers of retinal vasculature) in a way that does not accurately represent the anatomic reality.[14,16,24–26] In contrast, OCTA facilitates segmentation and visualization of vascular networks (manifested as areas with flow) in different retinal layers, permitting precise fractal analysis of each of these layers.

The advent of OCTA analysis can provide high resolution images that allow the visualization of morphologic microvascular abnormalities,[19,20,27–29] and also are well-suited to mathematical analysis of each vascular layer. Optical coherence tomography angiography parameters that have been reliably quantified in diabetic patients include the foveal avascular zone (FAZ), area of nonperfusion, and perfusion density.[19,29–33] Takase et al.[33] and Di et al.[32] showed statistically significant increases in the FAZ areas compared to controls in the superficial and deep capillary plexuses. De Carlo et al.[19] described similar changes of the FAZ, in addition to apparent remodeling of the FAZ and adjacent capillary nonperfusion in diabetic patients. Capillary nonperfusion and macular ischemia, seen in OCTA as areas of reduced flow, also may be quantified as markers of disease burden.[30]

The measurement of apparently absent or reduced perfusion in the different retinal layers is possible with OCTA. The analysis of vessel density is another promising approach to evaluate the degree of disease. Hwang et al.[30] and Agemy et al.[31] both show statistically significant reductions in vascular density in diabetic patients compared to controls using different approaches to calculate vascular density. In the latter study, the authors show a trend towards reducing vascular density with worsening severity of diabetic disease.[31]

The FD may be a helpful adjunct to these previously described quantifiable OCTA parameters of diabetic disease.[19,20,29,30,32,33] In addition, the reduction in FD in diabetics may better reflect the pathophysiologic loss of smaller vessels in diabetic retinopathy. In our study, we show significantly reduced FD values that also correspond to the reduction in the vascular density as measured by the Avanti automated software. Combining the FD and vascular density may allow

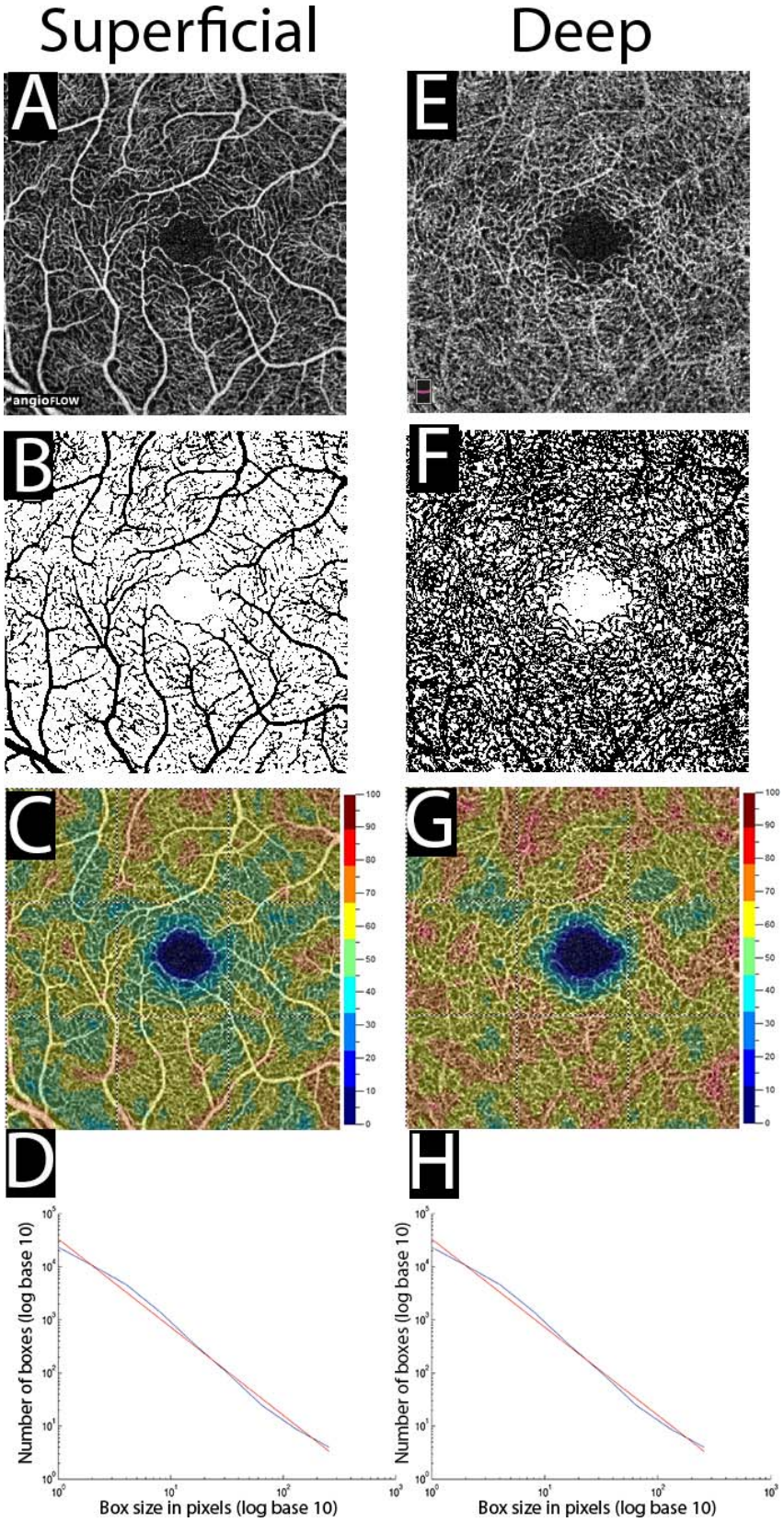

FIGURE 2. Right eye from a 29-year-old male from the control group. Superficial capillary plexus (*left column* from *top* to *bottom*): (**A**) Spectral-domain optical coherence tomography angiography image segmented through the superficial capillary plexus. (**B**) Spectral-domain optical coherence tomography angiography image after standardization, cropping, and binarization. (**C**) Vascular density analysis of the superficial capillary plexus (57.62%). (**D**) the FD for this image was determined to be 1.660. Deep capillary plexus (*right column* from *top* to *bottom*): (**E**) Spectral-domain optical coherence tomography angiography image segmented through the deep capillary plexus. (**F**) Spectral-domain optical coherence tomography angiography image after processing. (**G**) Vascular density analysis of the deep capillary plexus (62.93%). (**H**) The FD for this image was determined to be 1.794.

Investigative Ophthalmology & Visual Science

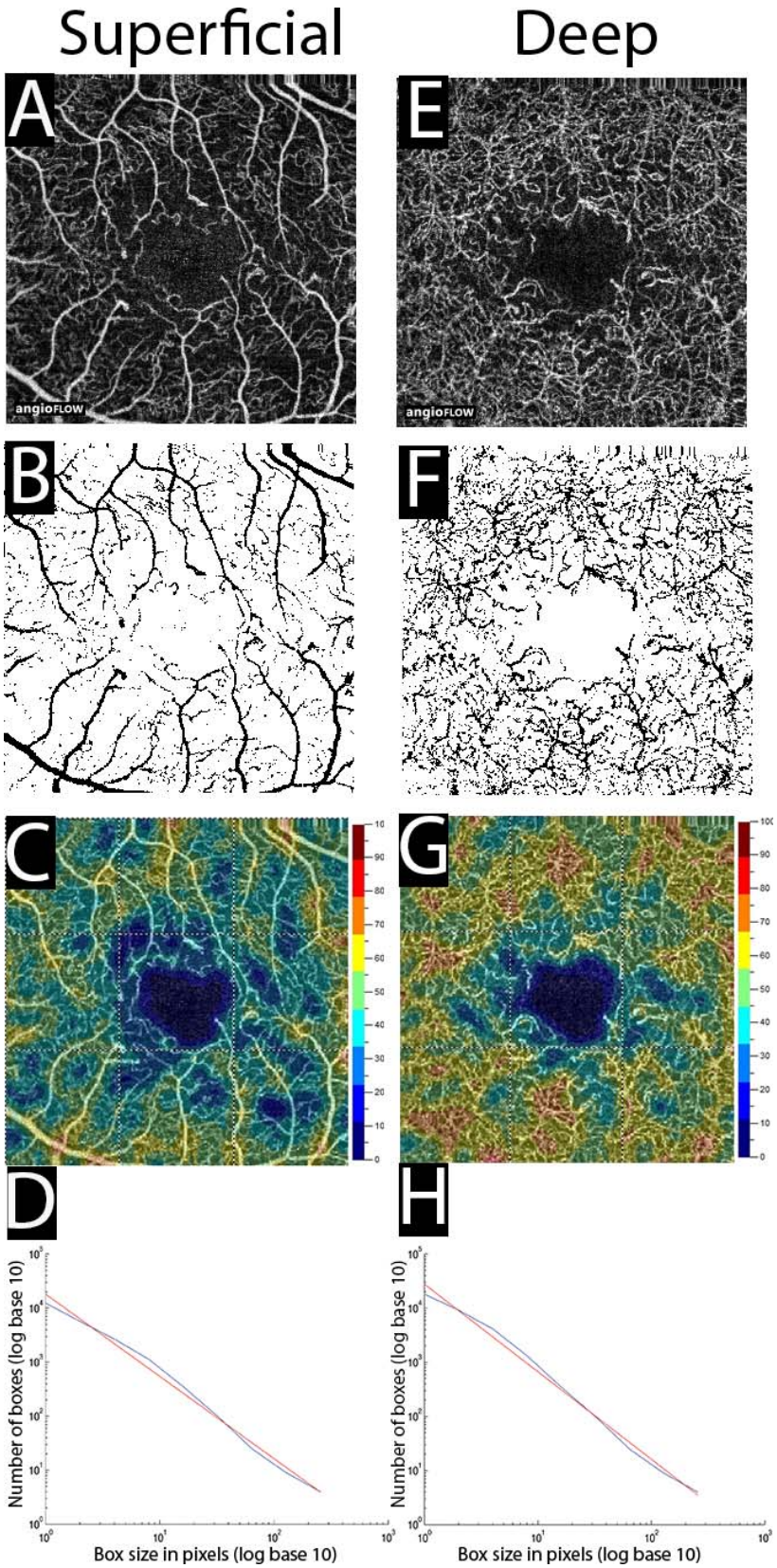

FIGURE 3. Left eye from a 37-year-old male patient in the diabetic group. Superficial capillary plexus (*left column* from *top* to *bottom*): (**A**) Spectral-domain optical coherence tomography angiography image segmented through the superficial capillary plexus. (**B**) Spectral-domain optical coherence tomography angiography image after standardization, cropping, and binarization. (**C**) Vascular density analysis of the superficial capillary plexus (42.86%). (**D**) The FD for this image was determined to be 1.521. Deep capillary plexus (*right column* from *top* to *bottom*): (**E**) Spectral-domain optical coherence tomography angiography image segmented through the deep capillary plexus. (**F**) Spectral-domain optical coherence tomography angiography image after processing. (**G**) Vascular density analysis of the deep capillary plexus (52.40%). (**H**) The FD for this image was determined to be 1.617.

Investigative Ophthalmology & Visual Science

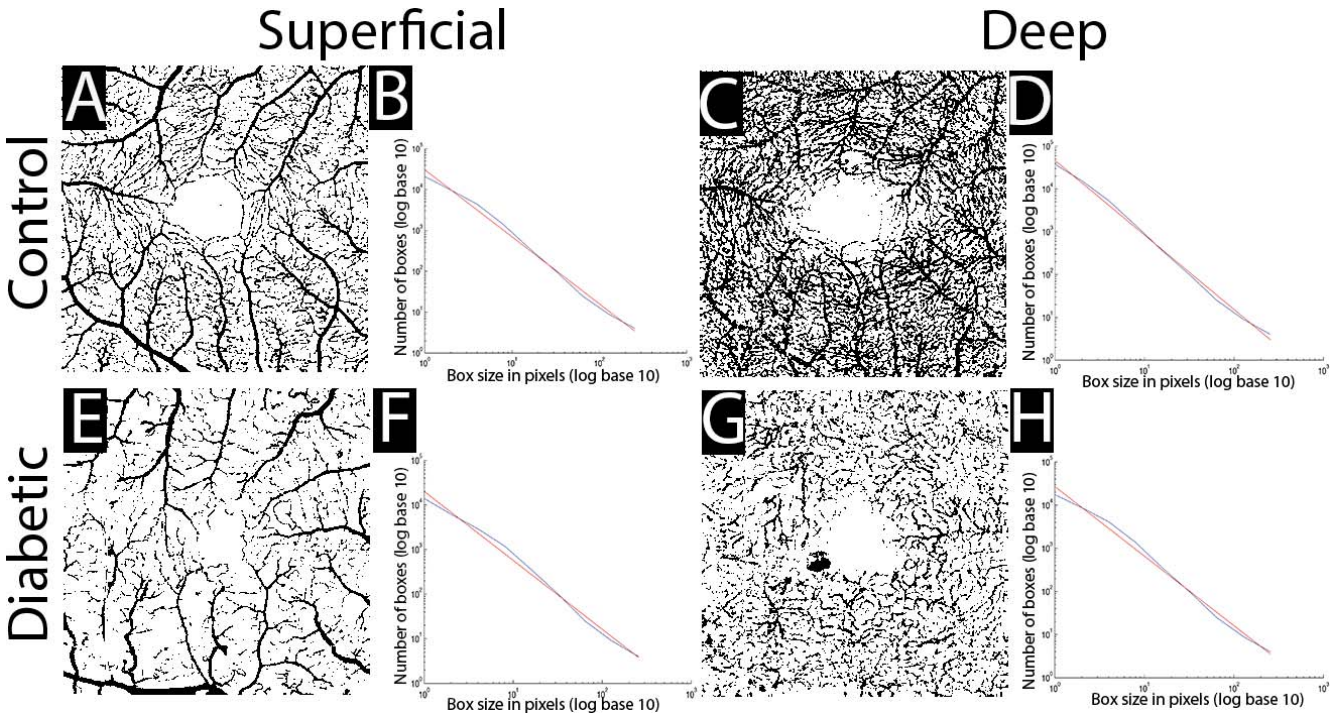

FIGURE 4. A 37-year-old in the control group (*top row left* to *right*): (**A**) Spectral-domain optical coherence tomography angiography image after processing of the right eye from a control subject segmented through the superficial capillary plexus. (**B**) The FD for this image was determined to be 1.639. (**C**) Spectral-domain optical coherence tomography angiography segmented through the deep capillary plexus. (**D**) The FD for this image was determined to be 1.739. A 52-year-old male patient in the diabetic group (*bottom row left* to *right*): (**E**) Spectral-domain optical coherence tomography angiography image after processing of the right eye from a diabetic patient segmented through the superficial capillary plexus. (**F**) The FD for this image was determined to be 1.545. (**G**) Spectral-domain optical coherence tomography angiography segmented through the deep capillary plexus. (**H**) The FD for this image was determined to be 1.612.

for a more nuanced assessment of microvascular disease. However, our small sample size may limit our ability to make meaningful conclusions regarding the most useful measures of disease severity in our cohort.

There are limitations to deploying fractal analysis to two-dimensional images of OCTA. Some of these limitations result from the numerous potential artifacts that can complicate OCTA imaging, including motion and projection artifacts, as well as automated segmentation failure.[34] Furthermore, the absence of vessels on OCTA does not confirm that vasculature is absent, as it is possible that the flow inside the vessels is lower than the threshold detectable by OCTA. Low flow would manifest as areas without vessels on OCTA imaging despite the actual anatomic presence of vessels (false-negative perfusion); this would be expected to artificially reduce the FD. We attempted to minimize the impact of artifacts on our analysis by excluding images with extensive motion artifact and patients with DME. A separate analysis of patients with diabetic retinopathy with DME demonstrated numerous artifacts producing artificially elevated FDs (data not shown). Furthermore, despite our selection/exclusion criteria, artifacts were nonetheless visible, as it was clear that projection artifacts were present with automated segmentation. We expect that these projection artifacts likely reduced the accuracy of our fractal calculations.

Our study has several weaknesses, including a small sample size and persistence of imaging artifacts, which may reduce the precision of fractal analysis. Furthermore, there was a large difference in mean age between the control and patient populations. It is possible that some of the difference observed in FD between these two groups resulted from age-related changes in the older diabetic patients. However, Gadde et al.[35] showed that the FD and vascular density did not change with age in healthy eyes. Despite these limitations, our finding of statistically significant reductions in the FD in diabetic eyes holds promise for the detection and monitoring of disease severity. This is important as analysis of the branching of vasculature is a more representative anatomic model than total vascular perfusion area in a given OCTA scan.

If our findings are consistent across multiple progressive stages of diabetic retinopathy, the FD may provide an objective means of monitoring disease severity as an adjunct to currently used grading criteria. Given that fractal geometry mirrors the physiologic branching of the retinal vascular tree, the FD may provide insights into our understanding of disease pathogenesis. Further work on a larger subset of diabetic patients (with age-matched controls), as well as application to three-dimensional reconstructions of OCTA and other imaging modalities, may reveal further insights.[27,36] We believe that fractal analysis is a clinically useful tool that may help guide follow-up and treatment for patients with more severe disease who are at greater risk of progression to proliferative disease or DME.

As this technology evolves and improves, the FD, combined with other quantitative measurements, such as the area of nonperfusion and vascular density, promise the possibility of pinpointing cutoffs for disease severity, risk stratification and monitoring of treatment response.

Acknowledgments

Supported by The Macula Foundation, Inc.

Disclosure: **S. Zahid**, None; **R. Dolz-Marco**, None; **K.B. Freund**, Optovue (C, R), Genentech (C, R), Optos (C, R), Bayer HealthCare

(C, R), Heidelberg Engineering (C, R); **C. Balaratnasingam**, None; **K. Dansingani**, None; **F. Gilani**, None; **N. Mehta**, None; **E. Young**, None; **M.R. Klifto**, None; **B. Chae**, None; **L.A. Yannuzzi**, None; **J.A. Young**, None

References

1. Goh JKH, Cheung CY, Sim SS, Tan PC, Tan GSW, Wong TY. Retinal imaging techniques for diabetic retinopathy screening. *J Diabetes Sci Technol*. 2016;10:282–294.
2. Ali Shah SA, Laude A, Faye I, Tang TB. Automated microaneurysm detection in diabetic retinopathy using curvelet transform. *J Biomed Opt*. 2016;21:101404.
3. Walton OB IV, Garoon RB, Weng CY, et al. Evaluation of automated teleretinal screening program for diabetic retinopathy. *JAMA Ophthalmol*. 2016;134:204–209.
4. Sun JK, Cavallerano JD, Silva PS. Future promise of and potential pitfalls for automated detection of diabetic retinopathy. *JAMA Ophthalmol*. 2016;134:210–211.
5. Virgili G, Menchini F, Casazza G, et al. Optical coherence tomography (OCT) for detection of macular oedema in patients with diabetic retinopathy. *Cochrane Database Syst Rev*. 2015;1:CD008081.
6. Reif R, Qin J, An L, Zhi Z, Dziennis S, Wang R. Quantifying optical microangiography images obtained from a spectral domain optical coherence tomography system. *Int J Biomed Imaging*. 2012;2012:509783.
7. Landini G, Misson GP, Murray PI. Fractal analysis of the normal human retinal fluorescein angiogram. *Curr Eye Res*. 1993;12:23–27.
8. de Mendonça MB de M, de Amorim Garcia CA, Nogueira R de A, Gomes MAF, Valença MM, Oréfice F. [Fractal analysis of retinal vascular tree: segmentation and estimation methods]. *Arq Bras Oftalmol*. 2007;70:413–422.
9. Jiang H, Debuc DC, Rundek T, et al. Automated segmentation and fractal analysis of high-resolution non-invasive capillary perfusion maps of the human retina. *Microvasc Res*. 2013;89:172–175.
10. Mainster MA. The fractal properties of retinal vessels: embryological and clinical implications. *Eye*. 1990;4:235–241.
11. Tălu S. Fractal analysis of normal retinal vascular network. *Oftalmologia*. 2011;55:11–16.
12. Masters BR. Fractal analysis of the vascular tree in the human retina. *Annu Rev Biomed Eng*. 2004;6:427–452.
13. Shin ES, Sorenson CM, Sheibani N. Diabetes and retinal vascular dysfunction. *J Ophthalmic Vis Res*. 2014;9:362–373.
14. Ţălu Ş, Călugăru DM, Lupaşcu CA. Characterisation of human non-proliferative diabetic retinopathy using the fractal analysis. *Int J Ophthalmol*. 2015;8:770–776.
15. Sng CCA, Wong WL, Cheung CY, Lee J, Tai ES, Wong TY. Retinal vascular fractal and blood pressure in a multiethnic population. *J Hypertens*. 2013;31:2036–2042.
16. Avakian A, Kalina RE, Sage EH, et al. Fractal analysis of region-based vascular change in the normal and non-proliferative diabetic retina. *Curr Eye Res*. 2002;24:274–280.
17. Spaide RF, Klancnik JM Jr, Cooney MJ. Retinal vascular layers imaged by fluorescein angiography and optical coherence tomography angiography. *JAMA Ophthalmol*. 2015;133:45–50.
18. Spaide RF, Fujimoto JG, Waheed NK. Optical coherence tomography angiography. *Retina*. 2015;35:2161–2162.
19. de Carlo TE, Chin AT, Bonini Filho MA, et al. Detection of microvascular changes in eyes of patients with diabetes but not clinical diabetic retinopathy using optical coherence tomography angiography. *Retina*. 2015;35:2364–2370.
20. Couturier A, Mané V, Bonnin S, et al. Capillary plexus anomalies in diabetic retinopathy on optical coherence tomography angiography. *Retina*. 2015;35:2384–2391.
21. Rasband WS. ImageJ, U. S. National Institutes of Health, Bethesda, Maryland, USA. Available at: http://imagej.nih.gov/ij/, 1997-2015. Accessed March 13, 2016.
22. Karperien A, Jelinek HF, Leandro JJG, Soares JVB, Cesar RM Jr, Luckie A. Automated detection of proliferative retinopathy in clinical practice. *Clin Ophthalmol*. 2008;2:109–122.
23. ThéMA (2014) Fractalyse—fractal analysis software. Available at: http://www.fractalyse.org. Accessed March 13, 2016.
24. Lee J, Zee BCY, Li Q. Detection of neovascularization based on fractal and texture analysis with interaction effects in diabetic retinopathy. *PLoS One*. 2013;8:e75699.
25. Daxer A. Characterisation of the neovascularisation process in diabetic retinopathy by means of fractal geometry: diagnostic implications. *Graefes Arch Clin Exp Ophthalmol*. 1993;231:681–686.
26. Daxer A. The fractal geometry of proliferative diabetic retinopathy: implications for the diagnosis and the process of retinal vasculogenesis. *Curr Eye Res*. 1993;12:1103–1109.
27. Matsunaga DR, Yi JJ, De Koo LO, Ameri H, Puliafito CA, Kashani AH. Optical coherence tomography angiography of diabetic retinopathy in human subjects. *Ophthalmic Surg Lasers Imaging Retina*. 2015;46:796–805.
28. Scarinci F, Jampol LM, Linsenmeier RA, Fawzi AA. Association of diabetic macular nonperfusion with outer retinal disruption on optical coherence tomography. *JAMA Ophthalmol*. 2015;133:1036–1044.
29. Ishibazawa A, Nagaoka T, Takahashi A, et al. Optical coherence tomography angiography in diabetic retinopathy: a prospective pilot study. *Am J Ophthalmol*. 2015;160:35–44.e1.
30. Hwang TS, Gao SS, Liu L, et al. Automated quantification of capillary nonperfusion using optical coherence tomography angiography in diabetic retinopathy. *JAMA Ophthalmol*. 2016:134:367–373.
31. Agemy SA, Scripsema NK, Shah CM, et al. Retinal vascular perfusion density mapping using optical coherence tomography angiography in normals and diabetic retinopathy patients. *Retina*. 2015;35:2353–2363.
32. Di G, Weihong Y, Xiao Z, et al. A morphological study of the foveal avascular zone in patients with diabetes mellitus using optical coherence tomography angiography. *Graefes Arch Clin Exp Ophthalmol*. 2016;254:873–879.
33. Takase N, Nozaki M, Kato A, Ozeki H, Yoshida M, Ogura Y. Enlargement of foveal avascular zone in diabetic eyes evaluated by en face optical coherence tomography angiography. *Retina*. 2015;35:2377–2383.
34. Spaide RF, Fujimoto JG, Waheed NK. Image artifacts in optical coherence tomography angiography. *Retina*. 2015;35:2163–2180.
35. Gadde SGK, Anegondi N, Bhanushali D, et al. Quantification of vessel density in retinal optical coherence tomography angiography images using local fractal dimension. *Invest Ophthalmol Vis Sci*. 2016;57:246–252.
36. Pinhas A, Razeen M, Dubow M, et al. Assessment of perfused foveal microvascular density and identification of nonperfused capillaries in healthy and vasculopathic eyes. *Invest Ophthalmol Vis Sci*. 2014;55:8056–8066.

Investigative Ophthalmology & Visual Science